JOURNAL OF CATALYSIS 31, 96–109 (1973)

A Simultaneous Infrared and Kinetic Study of the Reduction of Nitric Oxide by Carbon Monoxide over Copper Oxide

JACK W. LONDON* AND ALEXIS T. BELL

Department of Chemical Engineering, University of California, Berkeley, California 94720

Received March 8, 1973

Infrared spectroscopy has been used to observe the surface of a silica supported copper oxide catalyst during the reduction of nitric oxide by carbon monoxide. Spectra taken under reaction conditions show the presence of adsorbed CO, CO_2, NO, and N_2O as well as CO_3^{2-} and NO_3^- structures which characterize the degree of oxidation of the catalyst surface. An additional band observed at 2200 cm^{-1} and found only under reaction conditions has been assigned to an isocyanate structure of the form Cu^+NCO^-. The presence of this species together with other observations strongly supports the postulate that nitric oxide can dissociate upon adsorption.

By combining the spectral observations with measurements of the reaction kinetics, it has been possible to develop a reaction mechanism consisting of nine elementary steps. The principal assumptions of this mechanism are that NO dissociates upon adsorption, that N_2O acts as an intermediate to the formation of N_2, and that CO maintains the catalyst surface in a reduced state as well as competing for sites needed for the dissociation of NO. Based upon the proposed mechanism the rate of NO consumption can be expressed as

$$-r_{NO} = \frac{2b_1b_2C_{NO}}{(1 + b_2C_{NO} + b_3C_{N_2O})(1 + b_4C_{CO})}.$$

INTRODUCTION

The catalytic reduction of nitric oxide offers an attractive means for removing this material from automobile exhaust. Several recent reviews (*1–3*) have shown that hydrogen, carbon monoxide, and a variety of hydrocarbons can be used as reducing agents and that many transition metals and metal oxides can serve as catalysis. A system which has received particular attention is the reduction of nitric oxide by carbon monoxide. Studies performed on the reaction (*4–7*) have shown that copper oxide, chromium oxide, and copper chromite are among the more active catalysts and that at high temperatures and low to moderate reactor space times the only products observed are carbon dioxide and nitrogen. At lower temperatures and higher space times a third product, nitrous oxide, is formed (*8*).

Relatively little is known about the mechanism of the reaction between nitric oxide and carbon monoxide. Ayen and Ng (*5*) and Force and Ayen (*7*) have reported that the kinetics of the reaction carried out in the presence of copper chromite can be described by a rate expression derived from a single site mechanism which assumes that the rate limiting step is the reaction between adsorbed carbon monoxide and nitric oxide. Shelef and Kummer (*3*) have critized this mechanism because it assumes that both reactants adsorb on

* Present address: The Moore School of Electrical Engineering, University of Pennsylvania, Philadelphia, PA 19174.

a single site and because it fails to explain the formation of nitrous oxide. Based upon their work with chromia Shelef, Otto and Gandhi (*6*) have suggested that the reaction takes place by a sequential reduction and oxidation of the catalyst itself. The rate limiting step in this process is assumed to be the reoxidation of the catalyst by nitric oxide. It is noted further that in order for the catalyst to retain its activity, the surface chromium atoms must be maintained in a partially reduced state. In a separate investigation Shelef and Otto (*8*) have proposed that with catalysts such as Cu_2O and Co_3O_4 nitrogen may be produced by the heterogeneous decomposition of nitrous oxide, since these two catalysts have been observed (*9*) to be effective for this reaction.

The present investigation was undertaken to examine the mechanism of nitric oxide reduction by carbon monoxide over a copper oxide catalyst. Measurements were made of the reaction kinetics at the same time that infrared spectra were taken of the species adsorbed on the catalyst surface. The spectral results were interpreted with the assistance of the spectra taken for the individual adsorption of each reactant and product which were reported in the preceding paper (*10*). The spectral and kinetic data were then combined to develop a series of elementary steps which could explain all of the features observed experimentally.

Experimental Methods

The catalyst used for the present work was prepared by depositing copper oxide on a fine silica powder (Cab-O-Sil M-5) in such proportions that the final product contained 8.7% copper by weight. Details of the catalyst preparation may be found in Ref. (*10*). A small amount of the catalyst powder was pressed into a disc 1 in. in diameter, 0.03 in. thick, and weighing 0.200 g. In order to measure the disc temperature a small copper–constantan thermocouple was imbedded in the disc. A second disc containing only silica but with dimensions identical to those of the catalyst disc was also prepared. By placing the silica disc in the reference beam of the spectrometer and the catalyst disc in the sample beam it was possible to record the spectrum of species adsorbed on the catalyst and to subtract out the spectrum of the gas phase as well as the spectrum of species adsorbed on the silica support.

An overall view of the apparatus is

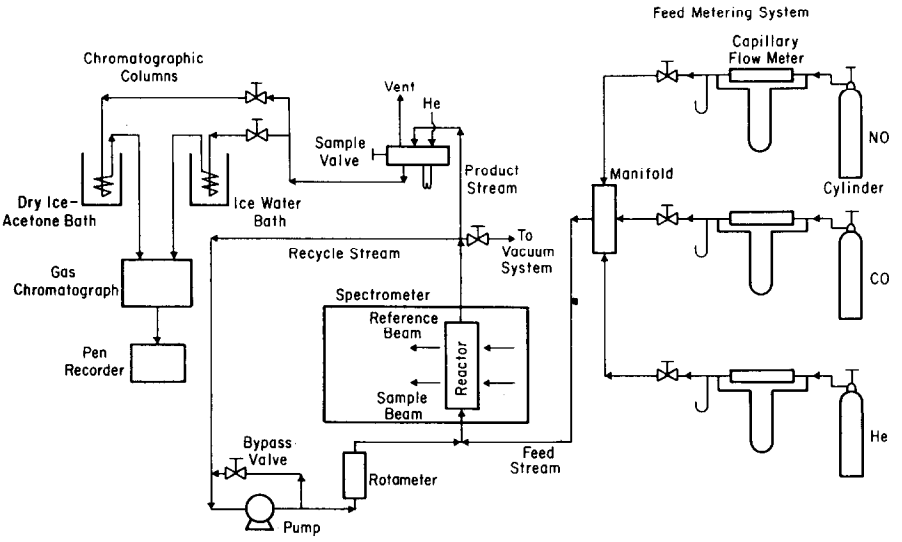

Fig. 1. Experimental apparatus.

shown in Fig. 1. The infrared cell described in the preceding paper (*10*) served as the reactor. The reactor was operated as part of a recycle loop in order to allow the measured reaction rates to be associated with a unique gas-phase composition. Circulation in the loop was maintained by a stainless steel bellows pump and was controlled by a bypass valve mounted between the inlet and outlet of the pump. The recirculation flow rate was measured by a rotameter. The flow rate of each reactant fed to the recycle loop was measured by a calibrated capillary flow meter and controlled by a micrometer metering valve. To maintain a constant delivery pressure, a low delivery pressure regulator was installed in each line between the gas-cylinder and the capillary flow meter.

The products taken from the recycle loop were analyzed by gas chromatography. Two columns operated in parallel were used to analyze for NO, CO, N_2O, N_2, and CO_2. Both columns were made of 20 ft long sections of ¼ in. stainless steel tubing packed with Porapak-Q. A switching valve permitted the helium carrier gas and sample to be passed through either one or the other column. The first column was maintained in a dry-ice–acetone bath at −78.5°C and served to separate N_2, NO, and CO. The heavier components N_2O and CO_2 were permanently adsorbed in this column. To avoid an excessive buildup of these components, the column was routinely brought up to room temperature and flushed with a flow of helium. The second column was maintained at 0°C in an ice water bath and was used to analyze for N_2O and CO_2. The light components came through this column as a single unresolved peak.

All of the measurements of reaction kinetics were carried out using a single catalyst disc. Each experimental run was initiated by recording the spectrum of the catalyst disc at 150°C in the presence of a vacuum of about 10^{-6} Torr. The vacuum was then broken with helium. At the same time the reactor heaters and the recycle pump were turned on. When the desired temperature level had been reached the flows of reactant gases were introduced. In order to determine the attainment of a steady state condition in the recycle loop, infrared spectra and gas chromatograms were taken until no further change could be observed in these two indicators. In practice, 2 to 3 hr were required to reach this condition.

For each run a minimum of three gas chromatographic analyses were performed for all components. An infrared spectrum was also recorded each time a gas analysis was made. At the end of a run the recycle loop was purged with helium for at least 1 hr. The reactor was then evacuated and maintained at 10^{-6} Torr and 150°C for at least 12 hr before the next run was begun.

Results

Infrared Spectra

Representative spectra of the catalyst disc taken under steady state reaction conditions are shown in Fig. 2. All of these spectra were recorded for runs in which carbon monoxide was present in excess of that required by the reaction stoichiometry. Five bands can be identified clearly, occurring at 2350, 2240, 2200, 2170, and 2140 cm^{-1}. In addition, two weaker bands can also be found. The first appears as a shoulder on the band at 2140 cm^{-1} and is centered near 2130 cm^{-1}. The second is a broad band centered at 1975 cm^{-1}.

The variation of band intensity with operating conditions is summarized in Table 1. Included in this table are the results of all of the conditions for which kinetic data were taken. As may be seen in Fig. 2 and Table 1 the strongest band observed is that at 2140 cm^{-1}. The intensity of this band decreases with increasing temperature for comparable mole fractions of CO and NO. At a fixed temperature and mole fraction of NO the intensity remains essentially constant even though the mole fraction of CO is increased almost twofold. For a fixed temperature and mole fraction of CO the variation of intensity with mole fraction of NO is more complex, the majority of cases indicating that the intensity passes

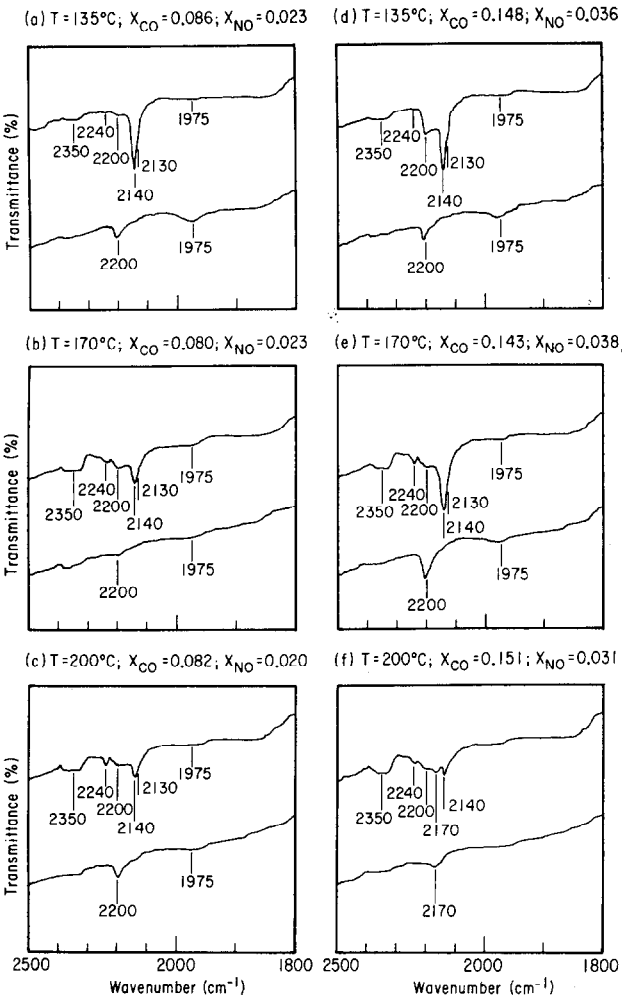

FIG. 2. Infrared spectra at steady state reaction conditions in the presence of excess CO.

through a minimum as the mole fraction of NO is increased. The second most intense band is that at 2200 cm^{-1}. The intensity of this band decreases slowly as the temperature is increased. For a constant temperature and mole fraction of NO there is a very noticeable increase in intensity with increasing mole fraction of CO. The response to an increase in mole fraction of NO at a constant temperature and mole fraction of CO is erratic and hence no general trend can be established. The band at 2170 cm^{-1} appears only in those spectra taken at 170 and 200°C. In a number of the spectra taken at these temperatures the band is not fully resolved and its presence can be identified only by the extended web formed between the bands at 2140 and 2200 cm^{-1}. The intensity of the band at 2170 cm^{-1} shows a definite increase with temperature for comparable mole fractions of CO and NO. At a constant temperature this band grows as either the mole fraction of CO is increased or the mole fraction of NO is decreased. The remaining bands occurring at 2350, 2240, and 1975 cm^{-1} show no definite trends with either temperature or mole fraction of either CO or NO.

In an attempt to determine the strength of adsorption of the species contributing to the steady state spectra shown in Fig.

TABLE 1
MAGNITUDE OF INFRARED BAND INTENSITIES

	Reactant and product mole fractions					Band depth						
T (°C)	x_{CO}	x_{NO}	x_{CO_2}	x_{N_2O}	x_{N_2}	2350	2240	2200	2170	2140	1975	Run no.
135	0.0863	0.0107	0.0032	0.0015	0.0008	1	<1	2	0	15	2	188
	0.0860	0.0170	0.0034	0.0016	0.0009	1	<1	4	0	13	2	198
	0.0860	0.0235	0.0035	0.0021	0.0007	1	<1	2	0	16	2	204
170	0.0803	0.0083	0.0087	0.0018	0.0035	1	<1	2	4	2	1	241
	0.0813	0.0162	0.0084	0.0029	0.0027	1	1	3	3	5	<1	247
	0.0800	0.0233	0.0101	0.0039	0.0030	1	<1	2	3	7	0	254
200	0.0855	0.0125	0.0065	0.0024	0.0020	2	1	1	3	2	—	298
	0.0825	0.0202	0.0071	0.0032	0.0019	2	1	2	3	6	<1	311
	0.0810	0.0323	0.0088	0.0042	0.0024	1	1	1	2	6	<1	321
135	0.1480	0.0144	0.0028	0.0013	0.0008	1	<1	3	0	17	2	229
	0.1480	0.0230	0.0030	0.0016	0.0007	<1	<1	4	0	16	5	221
	0.1463	0.0365	0.0032	0.0020	0.0006	<1	<1	7	0	15	3	214
170	0.1443	0.0185	0.0050	0.0026	0.0012	1	1	6	6	11	2	284
	0.1420	0.0233	0.0062	0.0032	0.0015	<1	<1	1	4	8	<1	276
	0.1433	0.0380	0.0079	0.0046	0.0017	2	<1	4	5	14	0	291
200	0.1475	0.0119	0.0045	0.0018	0.0014	1	<1	7	9	7	2	355
	0.1440	0.0310	0.0073	0.0029	0.0022	2	1	3	6	4	<1	345
	0.1410	0.0430	0.0075	0.0045	0.0015	1	2	3	5	9	2	363

2a–f, spectra were recorded after the termination of the reaction and evacuation of the gas phase. These spectra appear in the lower half of Fig. 2a–f and were recorded at the end of 12 hr during which the reactor was maintained at 10^{-5} Torr and 150°C. With the exception of the vacuum spectrum shown in Fig. 2f only two bands can be seen in these spectra, occurring at 2200 and 1975 cm^{-1}. The species which produce these bands are stable under vacuum and are not removed until a heated flow of helium is introduced into the reactor. The vacuum spectrum shown in Fig. 2f shows an additional band at 2170 cm^{-1}.

Figure 3 illustrates the spectra recorded under steady state conditions but in the presence of an excess of nitric oxide. The bands occurring between 2500 and 2000 cm^{-1} are identical to those seen in Fig. 2 but are greatly reduced in intensity. Three bands can also be seen at 1980, 1870, and 1565 cm^{-1}. The intensity of the central portion of the broad band centered at 1565 cm^{-1} decreases with increasing mole fraction of CO. The low frequency branch of the band, however, remains unaltered. This pattern suggests that the band ob-

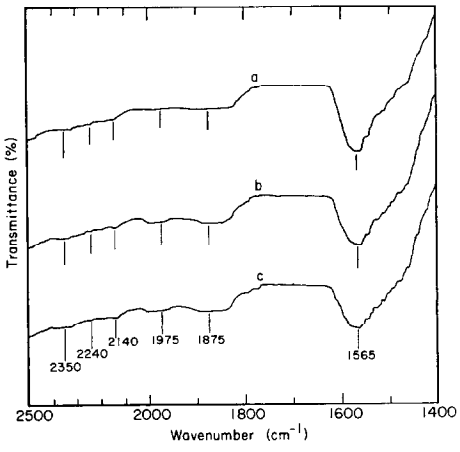

FIG. 3. Infrared spectra at steady state reaction conditions in the presence of excess NO: T = 135°C; (a) x_{CO} = 0.021, x_{NO} = 0.149; (b) x_{CO} = 0.030, x_{NO} = 0.149; (c) x_{NO} = 0.050, x_{CO} = 0.149.

served may be composed of two superposed bands, a very broad band and a somewhat narrower one which is sensitive to the mole fraction of CO.

In a series of experiments undertaken to clarify the reaction mechanism equimolar mixtures of carbon monoxide and nitric oxide were passed through the reactor without recirculation. Each experiment was initiated by bringing in one of the two reactant and allowing it to flow until a steady state spectrum could be observed. At this point the second reactant was introduced and the combined flow continued until a new steady state spectrum was obtained. Finally the flow of the first reactant was curtailed while the flow of the second reactant was continued. Spectra were then recorded until no further changes could be observed.

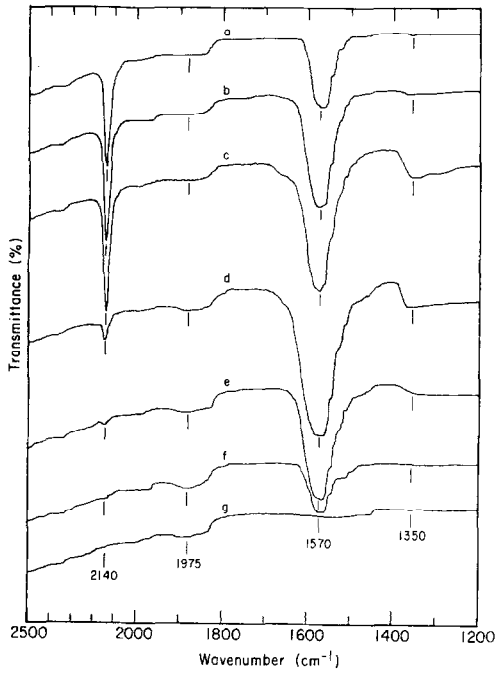

FIG. 4. Infrared spectra during reaction of CO and NO at 97°C: (a) 10 min after addition of CO, $x_{CO} = 0.05$; (b) 50 min after addition of CO, $x_{CO} = 0.05$; (c) 90 min after addition of CO, $x_{CO} = 0.05$; (d) 25 min after addition of NO, $x_{CO} = 0.05$ and $x_{NO} = 0.05$; (e) 55 min after removal of CO, $x_{NO} = 0.05$; (f) 80 min after removal of CO, $T = 127$°C and $x_{NO} = 0.05$; (g) 95 min after removal of CO, $T = 141$°C and $x_{NO} = 0.05$.

Figure 4 illustrates the sequence of spectra obtained at 97°C when CO is introduced first followed by CO and NO, and finally by NO alone. In the presence of CO alone three peaks appear at 2140, 1570, and 1350 cm^{-1} characteristic of adsorbed CO (*10*). With the addition of NO, the band at 2140 cm^{-1} is sharply reduced in intensity while those at 1570 and 1350 cm^{-1} are slightly increased. An additional feature which can be observed is the appearance of a weak band near 1975 cm^{-1}. When the flow of CO is stopped, the bands characteristic of adsorbed CO disappear from the spectrum leaving only the band at 1975 cm^{-1} characteristic of adsorbed NO (*10*).

The same sequence of events shown in Fig. 4 is repeated in Fig. 5 but for a temperature of 170°C. In this case, the spectrum for adsorbed CO shows two bands at 2170 and 2140 cm^{-1} but no bands at lower frequencies. Upon addition of the

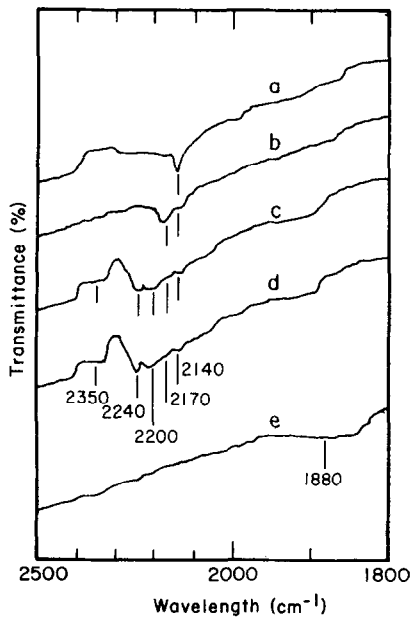

FIG. 5. Infrared spectra during reaction of CO and NO at 170°C: (a) 25 min after addition of CO, $x_{CO} = 0.05$; (b) 90 min after addition of CO, $x_{CO} = 0.05$; (c) 35 min after addition of NO, $x_{CO} = 0.05$ and $x_{NO} = 0.05$; (d) 155 min after addition of NO, $x_{CO} = 0.05$ and $x_{NO} = 0.05$; (e) 125 min after removal of CO, $x_{NO} = 0.05$.

NO, the bands for adsorbed CO are reduced in intensity and new bands appear at 2350, 2240, and 2200 cm^{-1}. The first two of these bands can be identified with CO_2 and N_2O (*10*). It should be noted that the inverted or positive adsorption bands at 2390 and 2300 cm^{-1} are caused by the presence of a greater gas-phase concentration of CO_2 on the reference side than on the sample side of the reactor. The concentration imbalance is produced by the lack of gas-phase mixing caused by using the reactor in its single pass mode. Finally, when only NO is allowed to flow the spectrum assumes the same form as that for NO adsorbed by itself at 170°C (*10*).

Figure 6 illustrates the spectra resulting when NO is introduced to the reactor first, followed by a mixture of NO and CO. In the presence of NO alone the only features observable are a weak band near 1880 cm^{-1} and a broad band in the vicinity of 1550 cm^{-1}. Addition of CO at 100°C causes the band at 1550 cm^{-1} to shift its position to 1565 cm^{-1}. At this temperature no bands can be observed for adsorbed CO, CO_2 or N_2O. Increasing the temperature to 135°C causes a decrease in the intensity of the band near 1565 cm^{-1} and the simultaneous growth of a band at 2140 cm^{-1} with a shoulder at 2130 cm^{-1}. In addition, two inverted bands at 2349 and 2224 cm^{-1} appear characteristic of gas-phase CO_2 and N_2O, respectively. Further increase in the temperature causes the band near 1565 cm^{-1} to disappear completely. The band at 2140 cm^{-1} at first grows slightly at the expense of the band at 1565 cm^{-1} but is reduced at higher temperatures. The gas-phase band for CO_2, which is initially smaller than that for N_2O, grows with increasing temperature, becoming more intense than the N_2O band at ~150°C. By contrast the N_2O band grows at first but above ~150°C begins to decrease so that at 170°C it is barely visible.

The effects of removing NO from the feed when the reactor is operating with recirculation are shown in Fig. 7. The first spectrum corresponds to a steady state at 135°C with CO in excess of NO. This spectrum

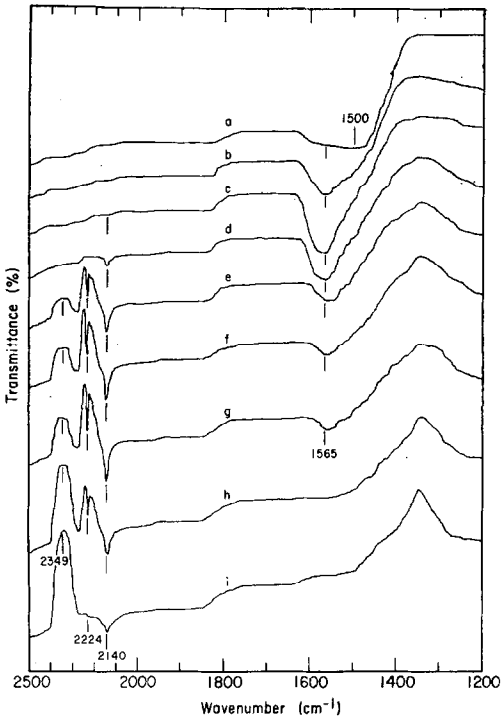

FIG. 6. Infrared spectra during reaction of CO and NO: (a) 3 hr and 5 min after addition of NO, T = 97°C and x_{NO} = 0.05; (b) 30 min after reaction with CO at T = 100°C, x_{CO} = 0.05 and x_{NO} = 0.05; (c) 7 hr and 55 min after reaction with CO at T = 100°C, x_{CO} = 0.05 and x_{NO} = 0.05; (d) 25 min after reaction temperature is increased to 125°C; (e) 25 min after reaction temperature is increased to 136°C; (f) 55 min after reaction temperature is increased to 136°C; (g) 2 hr and 40 min after reaction temperature is increased to 136°C; (h) 2 hr after reaction temperature is increased to 153°C; (i) 1 hr and 45 min after reaction temperature is increased to 167°C.

is quite similar to those shown in Fig. 2. When the NO feed is curtailed the bands at 2350, 2240, and 2140 cm^{-1} disappear leaving two bands at 2200 and 2130 cm^{-1}. Finally when the flow of CO is removed but the flow of helium is allowed to continue, only the band at 2200 cm^{-1} is retained. It should be noted that both the removal of NO and CO causes the intensity of the band at 2200 cm^{-1} to increase.

Kinetic Measurements

All of the measurements of reaction rates were performed with an excess of

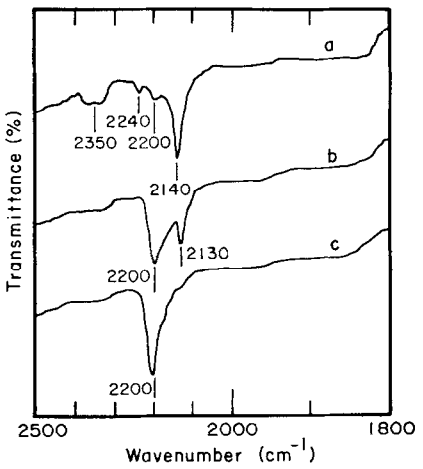

FIG. 7. Infrared spectra during reaction of CO and NO at 135°C: (a) steady state spectrum for a feed composition of $x_{CO} = 0.140$ and $x_{NO} = 0.075$; (b) 15 min after the cessation of NO flow; (c) 45 min after the cessation of CO flow.

either CO or NO so that the concentration of the reactant in excess could be assumed to be essentially constant. For those experiments in which CO was in excess runs were performed at 135, 170, and 200°C. At each temperature, the mole fraction of CO was maintained at approximately 0.085 or 0.145. The corresponding mole fractions of NO ranged from 0.005 to 0.035 and from 0.010 to 0.045 in order to insure that CO remained in at least a 2.5-fold excess. The balance of the gas fed to the reactor was helium which was used to establish a total pressure of 1 atm. In view of the relatively small concentrations of NO used, the total molar flow rate remained essentially constant at $\sim 3.8 \times 10^{-3}$ moles/min when the mole fraction of CO was 0.085 and $\sim 3.0 \times 10^{-3}$ moles/min when the CO mole fraction was 0.145. For the experiments in which NO was in excess runs were performed at 135°C only. The NO mole fraction was held constant at 0.145 and the total feed rate was $\sim 2.5 \times 10^{-3}$ moles/min.

The principal reason for using a recycle reactor was to achieve a high overall conversion at the same time that the per pass conversion could be maintained low enough for the catalyst disc to perform as a differential reactor. These conditions were achieved by maintaining the recycle ratio at about 70:1. A determination of the per pass conversion showed it to be a maximum of 2.5% and below 1% for most of the runs. At the same time the overall conversions ranged between 20 and 60%. Based on these figures it was concluded that the catalyst disc did in fact perform in a differential manner and that the reactor could be treated as a constant stirred tank reactor (*11*).

The only reaction products detected in the present studies were CO_2, N_2, and N_2O. Figure 8 shows the rates of product formation at 135°C as a function of the mole fraction of NO in the reactor for the case in which CO is in excess. It may be observed that while the rates of CO_2 and N_2O formation increase continually with increasing NO mole fraction, the rate of N_2 formation decreases. The data for 170 and 200°C are similar to those at 135°C except that the rate of N_2 formation exhibits an increase with increasing NO concentration. With an increase in the concentration of CO all of the rates are decreased.

The effect of temperature on the product composition is shown in Fig. 9. As may be seen the mole fraction of N_2 in the feed approaches a maximum near 200°C while the mole fractions of CO_2 and N_2O

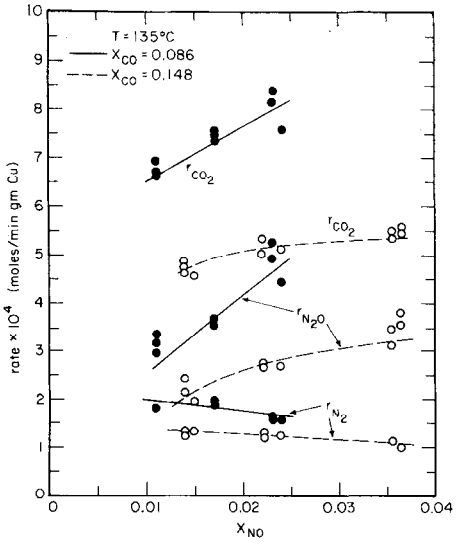

FIG. 8. Reaction rates at 135°C as a function of NO and CO mole fraction.

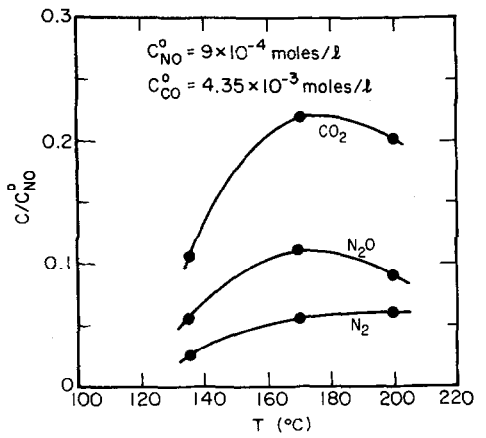

FIG. 9. Dependence of conversion on temperature.

pass through a maximum near 170°C. Similar patterns are exhibited by the spectra shown in Fig. 6.

For the runs in which NO was in excess, the reaction rates were too low to be measured with any accuracy. The chromatographic peaks for the products were so small that the peak heights were less than the noise level for the device.

DISCUSSION

Interpretation of Infrared Spectra

Most of the bands observed in Figs. 2–7 can be assigned to specific surface structures on the basis of the spectra obtained previously for the individual adsorption of CO, CO_2, NO, NA_2, and N_2O (*10*). A summary of the results of that study is shown in Table 2. Using Table 2 we can assign the bands at 2170, 2140, 1565 and 1350 cm^{-1} to CO; the band at 2350 cm^{-1} to CO_2; the bands at 1880 and 1550 cm^{-1} to NO; and the band at 2240 cm^{-1} to N_2O. Only the band for N_2O shows a significant shift from its position in the spectrum of N_2O adsorbed by itself. The assignment of the band at 2240 cm^{-1} to N_2O is supported by the correlation of its intensity with the gas-phase concentration of N_2O as seen in Table 1. Furthermore it should be noted that Zecchina, Cerruti and Borello (*12*) have observed a band at 2238 cm^{-1} for adsorbed N_2O attached through its oxygen end to chrome oxide. The remaining bands seen in Figs. 2–7 which occur at 2200, 2130, and 1975 cm^{-1} are unique to the spectra recorded under reaction conditions.

In attempting to identify the peaks responsible for the band at 2200 cm^{-1} it is helpful to review the conditions under which this band appears. Figure 2 shows that the band is present under steady

TABLE 2
VIBRATIONAL FREQUENCIES FOR ADSORBED CO, CO_2, NO, NO_2, AND N_2O

Adsorbate	Frequency (cm^{-1})	Structure
CO	2170	$M^-—CO^+$
	2140	M—CO
	1675	$M^+—OCO_2^-$
	1585–1565	$M^+—CO_2^-$
	1350	$M^+—OCO_2^-$
CO_2	2350	M—CO_2
NO	1890	$M^-{=}NO^+$ or $M^-{:}NO^+$
	1605	M—ONO_2 or M—ONO
	1575	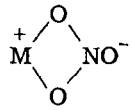
	1510	$M^+—ONO_2^-$
NO_2	1740	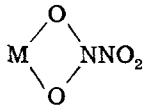
	1585	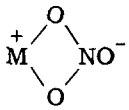
	1520	$M^+—ONO_2^-$
	1265	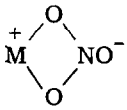
	745	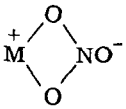
N_2O	2220	M—NNO or M—ONN

state reaction conditions when CO is in excess. Furthermore, the intensity of the band grows with increasing mole fraction of gas phase CO (see Table 1). When the gas phase is evacuated the band at 2200 cm^{-1} is retained, which suggests that the contributing surface species is relatively stable. The sequence of spectra seen in Fig. 6 shows that the band at 2200 cm^{-1} appears as soon as NO is added to a flow of CO but disappears when the flow of CO is stopped. Finally, the spectra shown in Fig. 7 demonstrate that the cessation of NO flow to a recirculating mixture of NO and CO causes the intensity of the 2200 cm^{-1} band to increase.

The circumstances under which the band at 2200 cm^{-1} is observed suggest that the responsible surface species is formed by an interaction between NO and CO. The possibility that the band is due to the adsorption of one of the final products can be ruled out by inspection of Table 2. Consequently, it must be assumed that the required surface structure is neither one of the reactants or products but rather some species containing at most atoms of C, N, and O. A review of the spectra of transition metal complexes shows that isocyanate complexes possess bands in the vicinity of 2200 cm^{-1} and that tetraethylammonium tetraisocyanatocuprate $(Et_4N)_2[Cu(NCO)_4]$ (*13*) exhibits a very strong band at 2198 cm^{-1} due to pseudo-antisymmetric stretching vibrations of NCO^-. The isocyanate groups also exhibits a weak band at about 1330 cm^{-1} due to pseudo-symmetric stretching vibrations. Based upon this evidence it is proposed that the band at 2200 cm^{-1} is best attributed to Cu^+NCO^-. The failure to observe a band near 1330 cm^{-1} does not rule out this assignment, since the transmission of the silica discs is very poor in this region of the spectrum.†

The band at 2130 cm^{-1} can be assigned to CO because of its proximity to the band at 2140 cm^{-1} and its dependence on the presence of gas-phase CO as seen in Fig. 6. The only previous observation of bands at this position is that of Seanor and Amberg (*14*) for a partially reduced copper oxide. This suggests that the band at 2130 cm^{-1} may be due to CO attached to a copper site present in a nonstoichiometric phase of copper oxide.

The band at 1975 cm^{-1} is very weak and appears only in those spectra taken under reaction conditions in the presence of excess CO. A band at this position has been observed for CO adsorption on NiO (*15–17*). However, the work of Roev and Alekseev (*18*) indicates that in the presence of NO the CO species contributing this band is removed. This observation and the absence of any bands near 1975 cm^{-1} during the adsorption of CO on copper oxide (*10*) lead us to rule out an assignment of this band to CO. Since adsorbed NO can form structures which vibrate below 2000 cm^{-1}, we believe that the band at 1975 cm^{-1} is most likely due to NO. Based upon Roev and Alekseev's (*18*) correlation of NO vibrational frequency with surface structure the band can be assigned to

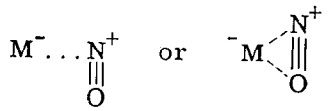

Since the band is not observed in the presence of excess NO, it suggests that the adsorption site is either Cu or Cu^+.

Reaction Mechanism and Kinetics

A reaction mechanism which is capable of explaining the formation of both N_2 and N_2O can be represented by the following nine elementary steps.

$$Cu + NO \rightleftarrows Cu\text{–}NO, \quad (1)$$

$$Cu\text{–}NO + Cu^+ \rightarrow Cu\text{–}N + Cu^{2+}O^-, \quad (2)$$

$$Cu\text{–}N + NO \rightarrow Cu + N_2O, \quad (3)$$

$$Cu^+ + CO \rightleftarrows Cu^+CO, \quad (4)$$

$$Cu + N_2O \rightleftarrows Cu\text{–}ONN, \quad (5)$$

$$Cu\text{–}ONN \rightarrow Cu^+O^- + N_2, \quad (6)$$

$$Cu^{2+}O^- + CO \rightarrow Cu^+ + CO_2, \quad (7)$$

$$Cu^+O^- + CO \rightarrow Cu + CO_2, \quad (8)$$

$$Cu\text{–}N + CO \rightleftarrows Cu^+NCO^-. \quad (9)$$

† Since the completion of this manuscript it has come to the authors' attention that Unland [*Science* **179**, 567 (1973)] has recently observed a stable isocyanate group attached to the surface of several transition metals.

This mechanism is also consistent with the spectral observations and leads to rate expressions which properly describe the reaction kinetics.

The selection of Cu and Cu^+ as the active catalytic sites is based on our observation as well as those of other (*4–7*) that the activity of copper oxide towards the reduction of NO by CO is enhanced when the catalyst surface is partially reduced. The spectra presented in Figs. 5 and 6 also support this conclusion since they show that the carbonates and nitrate structures characteristic of an oxidized surface are absent when the catalyst is active. The assumption that two types of reduced site are required stems from the mechanism by which NO is assumed to dissociate. This point is discussed below. Additional support for the requirement of both Cu and Cu^+ sites can be drawn from the work of Pierron, Rashkin and Roth (*19*) on the reaction of CO and O_2. Through an *in situ* analysis of the catalyst composition by X-ray diffraction it was demonstrated that the most active forms of CuO contained high levels of both Cu and Cu_2O under reaction conditions. In view of these results it was suggested that the active sites for CO reduction might be located at the boundary between the two reduced phases.

As indicated by reaction 2 it is postulated that NO dissociates upon adsorption. The principal support for this postulate is the observation of an isocyanate species in the infrared spectra shown in Figs. 2, 6, and 7. The presence of this species strongly suggests that NO dissociates, producing an adsorbed nitrogen atom which can subsequently react with a molecule of CO to produce the isocyanate group (reaction 9). Further evidence for NO dissociation can be derived from the fact that after operation under reducing conditions the catalyst can be oxidized to its less active form by exposing the catalyst disc to a heated stream of NO. It would seem reasonable to expect that the reoxidation of the reduced sites on the catalyst surface would occur via the dissociation of adsorbed NO.

The spectra shown in Figs. 2–7 indicate that only two bands can be observed for adsorbed NO. The first of these bands, occurring at 1975 cm^{-1}, has been ascribed to an ionic structure in which the axis of NO^+ is parallel to the plane of the catalyst surface. Because the vibrational frequency of the N–O bond is shifted upscale from that for gaseous NO (1876 cm^{-1}) this indicates a strengthening of the bond. As a result the band at 1975 cm^{-1} cannot be associated with the precursor to NO dissociation. This conclusion is further supported by the observation that this band is stable under vacuum. The second band occurs at 1880 cm^{-1} and is only slightly shifted in position from that for gaseous NO. The structure contributing this band is weakly attached to the surface and is readily removed under vacuum. Consequently, it appears more reasonable to propose that this form of adsorbed NO is the one which dissociates.

The selection of Cu as the adsorption site for NO, and Cu^+ as the recipient of the O atom produced through the dissociation of NO is based on the following reasoning. In order for the N–O bond to be broken it is anticipated that it will be necessary to first weaken the bond through the addition of an electron into the antibonding orbital of the N–O bond. Adsorption on a Cu site should facilitate this step since it should be easier to withdraw an electron from Cu than from Cu^+. Whereas either Cu or Cu^+ could act as the recipient for the O atom released upon dissociation of NO, the latter has been chosen in view of the mechanism by which CO is expected to inhibit the reduction of NO. According to reaction 4, CO competes for one of the sites required for NO dissociation. Based upon the absence of any bands near 2110 cm^{-1} characteristic of CO adsorption on Cu (*10*) it is concluded that CO adsorbs only on Cu^+ and possibly Cu^{2+}. Thus it seems reasonable to conclude that Cu^+ rather than Cu acts as the recipient of the oxygen atom and that the inhibition of NO reduction by increased CO partial pressures is caused by the adsorption of CO on these sites.

Additional support for Cu^+ as the adsorption site for CO is given by the se-

quence of spectra shown in Figs. 4 and 5. In the absence of NO a strong band can be observed at 2140 cm^{-1}. When NO is added to the feed the intensity of this band is strongly reduced. If one assumes that CO is preferentially adsorbed on Cu^+ sites, then the addition of NO must be interpreted as causing a reduction in the number of Cu^+ sites. This interpretation is completely consistent with the observation that the oxidation state of the copper oxide surface depends upon the relative amounts of CO and NO present in the gas phase.

An alternative to reaction 2 which could also explain the presence of surface nitrogen atoms can be expressed as

$$MNO + MCO \rightarrow MN + CO_2, \quad (2a)$$

in which M could be either Cu or Cu^+. For CO to act as an inhibitor of NO reduction the adsorption site M would have to be the same for both NO and CO. A mechanism built up around reaction 2a was considered but discarded when it was found that the rate expressions developed from this mechanism could not be fitted to the kinetic data.

It has been observed by Shelf and Otto (*8*) that N_2O is formed when the reaction temperature is low and that the ratio of N_2O to N_2 found in the products is sensitive to the reactor space time. These observations are confirmed in the present work and suggest that N_2O is in fact an intermediate product which is further reduced to N_2 at higher temperatures and longer space times. Reactions 3, 5, and 6 offer a plausible means for explaining this role of N_2O. By the manner in which these reactions have been written it is implied that the adsorption of N_2O through its nitrogen end is weaker than adsorption through its oxygen end. Although direct evidence for this behavior was not observed in the present study, such a conclusion has been deduced by Zecchina, Cerruti and Borello (*12*) for N_2O adsorption on chromia.

A number of alternatives to reactions 3, 5, and 6 were also considered, among these being

$$M\text{-}NO + M\text{-}NO \rightarrow M^+O^- + N_2O + M, \quad (3a)$$
$$M\text{-}N + M\text{-}NO \rightarrow N_2O + 2M \quad (3b)$$

for the formation of N_2O and

$$M\text{-}ONN + M\text{-}CO \rightarrow N_2 + CO_2 + 2M, \quad (6a)$$
$$M\text{-}N + M\text{-}N \rightarrow N_2 + 2M \quad (6b)$$

for the formation of N_2. Since NO is known (*20*) to interact with transition metals through its nitrogen end, reaction 3a was ruled out because of the steric problems anticipated in forming N_2O. Reaction 3b is not sterically hindered and hence could represent a valid step. To the extent that such a reaction could occur without perturbing the concentration of adsorbed NO, the rate expression for N_2O formation derived by its substitution into the mechanism would have an identical dependence on gas-phase concentrations as that derived by using reaction 3. Neither reaction 6a or 6b could be ruled out on an a priori basis. On the other hand their

TABLE 3

VALUES OF b_1, b_2, b_3, b_4, AND b_5 DERIVED BY FITTING $-r_{NO}$ AND r_{N_2} TO THE KINETIC DATA

T (°C)	b_1	b_2	b_3	b_4	Av absolute relative deviation (%)	b_5
135	0.011	2403	0	4392	4.21	9.2 8.3
170	0.023	2942	0	2103	10.12	19.3 8.0
200	0.012	2137	0	2098	4.02	11.8 9.5
135	0.011	3400	1000	4400	4.98	
170	0.023	2942	1000	4103	10.07	
200	0.012	2102	781	1956	4.15	

inclusion into the mechanism led to rate expressions which could not be fitted to the data.

Reaction steps 7 and 8 provide a path for restoring the Cu and Cu^+ sites consumed by interactions with NO and N_2O. Whereas these two reactions have been written under the assumption that gaseous CO reacts directly with the adsorbed oxygen atoms, it is possible that the reaction might require the prior adsorption of CO on a metallic site. Provided the subsequent reaction between the adsorbed CO and O did not significantly disturb the CO adsorption equilibrium both reduction paths would be indistinguishable. In view of this we have selected the simpler of the two alternatives.

Based upon the proposed mechanism the following expressions can be obtained for the rates of N_2O and N_2 formation

$$r_{N_2O} = \frac{k_2K_1\bar{C}_{Cu}\bar{C}_{Cu^+}C_{NO}}{[1 + K_1C_{NO} + (K_9k_2K_1\bar{C}_{Cu^+}/k_3K_4) + K_5C_{N_2O}](1 + K_4C_{CO})} - \frac{k_6K_5\bar{C}_{Cu}C_{N_2O}}{[1 + K_1C_{NO} + (K_9k_2K_1\bar{C}_{Cu^+}/k_3K_4) + K_5C_{N_2O}]}$$

$$r_{N_2} = \frac{k_6K_5\bar{C}_{Cu}C_{N_2O}}{[1 + K_1C_{NO} + (K_9k_2K_1\bar{C}_{Cu^+}/k_3K_4) + K_5C_{N_2O}]},$$

where C_x is the gas-phase concentration of component x, $\bar{C}_{Cu}$ and $\bar{C}_{Cu^+}$ are the concentrations of Cu and Cu^+ sites, respectively, on the catalyst surface, k_i is the rate constant for reaction i, and K_i is the equilibrium constant for reaction i. These rate expressions were fitted to the kinetic data by a nonlinear regression technique. It was found on the basis of experience that the ability of the nonlinear regression algorithm to fit the data deteriorated as either the complexity of the fitting function, the number of variables, or the number of fitted parameters was increased. To minimize these difficulties, the rates of N_2O and N_2 formation were added to obtain the expression

$$-\frac{1}{2}r_{NO} = r_{N_2O} + r_{N_2} = \frac{b_1b_2C_{NO}}{(1 + b_2C_{NO} + b_3C_{N_2O})(1 + b_4C_{CO})},$$

where $b_1 = k_2K_1\bar{C}_{Cu}\bar{C}_{Cu^+}/Q$, $b_2 = K_1/Q$, $b_3 = k_6K_5/Q$, $b_4 = K_4$, and $Q = 1 + K_9k_2K_1\bar{C}_{Cu^+}/k_3K_4$.

The results obtained from the regression analysis are shown in Table 3 and Fig. 8. As may be seen from Table 3, the best fit to the data is obtained when $b_3 = 0$. Since this result imples that N_2O does not adsorb on the catalyst surface, it is in conflict with the spectral observation of adsorbed N_2O. In an effort to explore the effects of making b_3 small but nonzero, its value was increased slowly. What was observed was an insignificant change in the relative deviations until the values of b_3 reached the level shown in the bottom half of Table 3. Above these values, the relative deviations increased rapidly. From these observations it was concluded that $b_3C_{N_2O} \ll 1 + b_2C_{NO}$ and hence that the concentration of adsorbed N_2O is small.

The constant b_4 is equal to K_4, the adsorption equilibrium constant for CO, and is the only one of the five constants for which it is possible to offer a direct physical interpretation. The values of b_4 shown in Table 3 exhibit the proper behavior for an equilibrium constant, increasing with decreasing temperature. From a plot of ln b_4 versus $1/T$ it was deduced that the corresponding heat of adsorption for CO is 5.2 kcal/mole. This value is considerably lower than that observed by Stone (*21*) for CO adsorption on Cu_2O (20 kcal/mole) and lies somewhat closer to the values observed by Smith and Quets (*22*) (10–20 kcal/mole) for CO adsorption on metallic copper. In the light of the limited data available from the present study no further explanation can be offered concerning this discrepancy.

An additional test of the proposed mechanism was obtained by examining the rate

of N_2 formation. For this purpose r_{N_2} is written as

$$r_{N_2} = \frac{b_5 C_{N_2O}}{(1 + b_2 C_{NO} + b_3 C_{N_2O})}$$

where $b_5 = k_6 K_5 \tilde{C}_{Cu}/Q$. Using the values of b_2 and b_3 listed in Table 3 and the experimental values of r_{N_2}, C_{NO}, and C_{N_2O}, a value of b_5 was calculated for each run. A summary of these calculations is shown in Table 3. For each temperature two values of b_5 are shown. The upper value corresponds to a nominal CO mole fraction of 0.085 and the lower value to a nominal CO mole fraction of 0.145. For a given temperature and mole fraction of CO, b_5 showed relatively little variation with the mole fraction of NO. On the other hand a definite correlation of b_5 with CO mole fraction could be observed. Although a satisfactory explanation of this variation cannot be given at this time, it should be noted that the difference between the two values of b_5 calculated for a given temperature is greatly reduced when the fit to the kinetic data is good. Thus a comparison of the results for 135 and 200°C with those for 170°C shows that the smaller the value of the absolute relative deviation the smaller will be the difference in the values of b_5.

In conclusion, the mechanism comprised of reactions 1–9 provides a plausible interpretation for all of the qualitative features of the kinetic data. The surface structures required by this mechanism have been shown to be consistent with the observations of the surface made by infrared spectroscopy. Finally, it has been demonstrated that the reaction rate expressions derived from the mechanism can be fitted to the kinetic data.

Acknowledgment

This work was supported by the National Science Foundation under Grants GK-4577 and GK-29162.

References

1. Caretto, L. S., McElroy, M. W., Nelson, J. L., and Venturini, P. D., *in* "Project Clean Air Task Force Assessments," Vol. 1, prepared for the University of California, Sept. 1, 1970.
2. Dwyer, F. G., *Catal. Rev.* **62**, 261 (1972).
3. Shelef, M., and Kummer, J. T., *Chem. Eng. Progr., Symp. Ser.* **67**, No. 115 (1972).
4. Baker, R., and Doerr, R., *Ind. Eng. Chem. Process Des. Develop.* **4**, 189 (1965).
5. Ayen, R. J., and Ng, Y., *Air Water Pollut.* **10**, 1 (1966).
6. Shelef, M., Otto, K., and Gandhi, H., *J. Catal.* **12**, 361 (1968).
7. Force, E. L., and Ayen, R. J., *Chem. Eng. Progr., Symp. Ser.* **68**, No. 126 (1973).
8. Selef, M., and Otto, K., *J. Catal.* **10**, 408 (1968).
9. Stone, F., *in* "Chemisorption" (W. Garner, Ed.), p. 179. Butterworths, London, 1957.
10. London, J. W., and Bell, A. T., *J. Catal.* **31**, 32 (1973).
11. Vosolsabě, J., and Michálek, J., *Collect. Czech. Chem. Commun.* **31**, 2646 (1966).
12. Zecchina, A., Cerruti, L., and Borello, E., *J. Catal.* **25**, 55 (1972).
13. Foster, D., and Goodgame, D. M. L., *J. Chem. Soc., London* 262 (1965).
14. Seanor, D. A., and Amberg, C. H., *J. Chem. Phys.* **42**, 2967 (1965).
15. Eischens, R. P., and Pliskin, W. A., *in* "Advances in Catalysis" (D. D. Eley, W. G. Frankenburg, V. I. Komarewsky, and P. W. Weisz, Eds.), Vol. 9, p. 662. Academic Press, New York, 1957.
16. Courtois, M., and Teichner, S. J., *J. Catal.* **1**, 121 (1962).
17. Alexeyev, A., and Terenin, A., *J. Catal.* **4**, 440 (1965).
18. Roev, L. M., and Alekseev, A. V., *in* "Elementary Photoprocesses in Molecules" (B. S. Neporent, Ed.; Engl. transl.), p. 260. Consultants Bur. New York, 1968.
19. Pierron, E. D., Rashkin, J. A., and Roth, J. F., *J. Catal.* **9**, 38 (1967).
20. Roev, L. M., and Zasuha, V. A., Teor. Eksp. Khim. **6**, 614 (1970).
21. Stone, F. S., *in* "Advances in Catalysis" (D. D. Eley, P. W. Selwood, and P. B. Weisz, Eds.), Vol. 13, p. 1. Academic Press, New York, 1962.
22. Smith, A. W., and Quets, J. M., *J. Catal.* **4**, 163 (1965).